

## Article

# Design of Cost-Effective and Sustainable Treatments of Old Landslides Adapted to the Moroccan Road Network: A Case Study of Regional Road R410 Crossing the Rifan Structural Domain

Omar Inabi <sup>1,\*</sup>, Mustapha Attou <sup>2</sup>, Mostafa Benzaazoua <sup>1</sup>  and Mohamed Qachar <sup>3</sup>

<sup>1</sup> Geology and Sustainable Mining Institute, Mohammed VI Polytechnic University (UM6P), Benguerir 43150, Morocco

<sup>2</sup> Conseil, Ingénierie et Développement (CID), Sale 11100, Morocco

<sup>3</sup> Department of Studies, Development and Road Research at the General Direction of Roads, Rabat 10100, Morocco

\* Correspondence: omar.inabi@um6p.ma

**Abstract:** The Moroccan road network is susceptible to multiple landslides annually, particularly in the northern regions due to high rainfall and specific geology. These events result in significant economic and social negative consequences, highlighting the need for sustainable and cost-effective solutions for network maintenance. This study outlines the methodology employed in addressing the issues within the RR410 regional road (Rifain region of Morocco), which entailed a thorough examination of the malfunctions, specific surveys, laboratory testing, and problem modeling. By incorporating long-term test-derived shear strength parameters, the model indicated that the road platform was stable, and back analysis using TALREN 4 software allows for model calibration. At kilometric point 23, using earthwork-based solutions (e.g., purging and replacing the base layer, employing granular water-insensitive substitution material) was found to provide a sustainable alternative to the expensive reinforced concrete-based solutions commonly used. Furthermore, these solutions contributed to the use of environmentally friendly and locally sourced materials. Road alignment rectification to anchor the platform in suitable soil was also an effective solution, as demonstrated at kilometric point 48. Additionally, enhancing the drainage and sanitation infrastructure, such as installing draining trenches, spurs, and reinforcing existing water structures, is a crucial aspect of addressing most landslides in the region.

**Keywords:** landslide treatment; road geotechnics; back analysis; sustainability



**Citation:** Inabi, O.; Attou, M.; Benzaazoua, M.; Qachar, M. Design of Cost-Effective and Sustainable Treatments of Old Landslides Adapted to the Moroccan Road Network: A Case Study of Regional Road R410 Crossing the Rifan Structural Domain. *Water* **2023**, *15*, 2423. <https://doi.org/10.3390/w15132423>

Academic Editors: Zizheng Guo, Samuele Segoni and Yixiang Song

Received: 8 June 2023

Revised: 27 June 2023

Accepted: 28 June 2023

Published: 30 June 2023



**Copyright:** © 2023 by the authors. Licensee MDPI, Basel, Switzerland. This article is an open access article distributed under the terms and conditions of the Creative Commons Attribution (CC BY) license (<https://creativecommons.org/licenses/by/4.0/>).

## 1. Introduction

Landslides are more common than any other geological phenomenon and can occur anywhere in the world. They occur when large masses of soil, rock, or debris move down a slope because of natural phenomena or human activity. Mud or debris flows are also a common type of fast-moving landslide [1]. Most landslides are natural phenomena affected by landscape development and are determined by trigger mechanisms mainly related to rain or earthquakes. In addition to their economic impact [2], landslides dramatically impact human life around the world every year [3,4]. Similarly, the expected increasing frequency and intensity of extreme rainfall events, coupled with population growth, deforestation, rapid urbanization, and unplanned development in landslide-prone areas, is likely to result in increased landslide fatalities worldwide [3,4].

In the Kingdom of Morocco, as in several regions of the world, field instabilities are one of the most serious problems on several levels: social, economic, and environmental [5]. Located in the north of the kingdom, the Rifan structural domain has specific geomorphological, geological, climatological, and geotechnical characteristics [6]. Every

year, several landslides occur on the road network due to important and irregular rainfalls. They have variable impacts, which affect the environment of the road et al.o impact the infrastructure itself. These landslides are unexpected events and the cost of repairing them is often not preplanned by the network managers. Therefore, traffic along these road links may therefore be disrupted or even cut off, hence the need to intervene quickly to restore traffic.

In this context, many different methods are usually used to investigate landslides and to study the stability of slopes. Usual slope stability analysis consists of the slices method, Bishop's method of slices, kinematic analysis, and limit equilibrium analysis [7]. For modeling, the most common method for calculating the safety factor is Bishop's simplified method [8]. Several comparative studies between classical limit equilibrium [9] and finite element methods [10] have shown that the results obtained remain very close [11–18]. Also, Mansour et al. [19] used 135 different slopes configurations and calculate their safety factors, using different methods, such as Spencer, Janbu (corrected), and Bishop simplified. A comparison with the results of finite difference method (FDM) was made, which showed that all mentioned methods had very close results.

Moreover, several studies have been conducted around the world to investigate the causes, triggering factors, damage, and potential landslide prevention measures. The first parameter that emerges in the majority of studies is the shear strength of the landslide matrix material, which is required [20]. Also, water is a common factor in most landslides. According to Li et al. [21], at 7% moisture content in Malan Loess in China, the shear strength parameters (cohesion and angle of friction) are at their maximum value, which reduces to 20% moisture content, and after this, cohesion decreases extremely, and material starts to slide. Zhang et al. [22] used a direct shear test to determine the mechanism of failure of red mudstone and the test results showed that increasing the degree of saturation from 48% to 100% reduced the value of mudstone cohesion by 26% and the angle of internal friction by 52%. Furthermore, submerging samples in water for 16 days at the same saturation level reduced the angle of internal friction and cohesion by 69% and 77%, respectively.

Ahmed et al. [23] investigated the failure analysis of a rainfall-triggered Havelian landslide in Pakistan. A series of direct shear tests were performed on reconstituted samples at in situ landslide matrix material density with varying degrees of saturation. Finally, the FOS along the likely surface failure was calculated using shear strength parameters at different degrees of saturation. The study discovered that as the degree of saturation of the soil matrix increased, the shear strength decreased, and the slope became critical at about 50% saturation.

In addition, several researchers [24–31] have examined the application of physical or empirical models on the impact of precipitation on slope stability. Most of them claimed that the effects of meteorological, morphological, and geological characteristics were mitigated. Lazzari et al. [32] were able to show how intense rainfall affected the frequency and occurrence of landslides. This is particularly true in steep and clay soil areas. Therefore, it may be concluded that rainfall has a significant role in the incidence of slope instability in the Thohoyandou areas.

For convenience reasons, this paper presents the cases of two unstable areas, namely kilometric point 23 and 48, within a problematic road in the north of Morocco, which would represent the most recurrent damage in a similar environment. While the study itself focused on about ten unstable sections. The main aim of this work is to share an experience on an axis where several field instabilities are developing, to describe the methodology adopted, the results obtained, and the lessons learned.

## 2. Study Area

### 2.1. Location

The study area is located in the northeast mountainous chain of the province of El Ksar El Kbir.

The R410, as shown in the Figure 1, is a regional road that starts at the city of Ksar EL Kebir and ends on national road RN13 at the town of Derdara. It plays a very important role in the Moroccan road network, as it directly connects the two provinces of Larache and Chefchaouen, passing through several rural centers and municipalities. According to the collection of road traffic, published annually by the Ministry of Equipment and Water (refer to the website of the ministry), the average annual daily traffic was around 2200 vehicles per day during the year 2014. This shows the importance of this road axis.

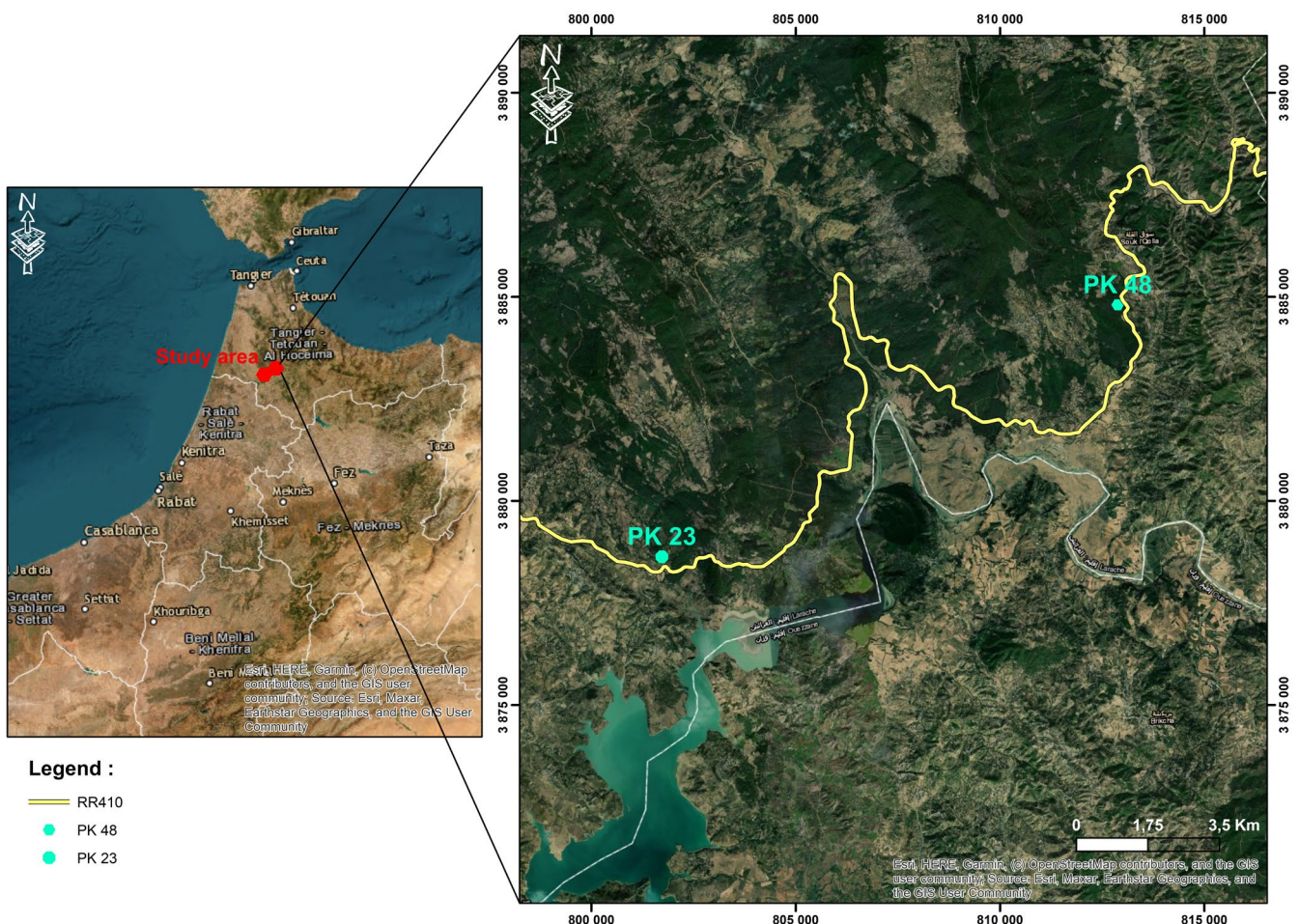


**Figure 1.** Location map of the RR410 road and the sections studied.

## 2.2. Geological Context of the Study Area

The study area belongs to the Rifan domain, which is a geological region located in the northern part of Morocco, and it is part of the western Mediterranean orogenic belt. The geology of the Rifan domain is complex and has been influenced by several tectonic events throughout its history, which has resulted in a diverse range of rocks and geological structures.

From a geological point of view, the region of Ksar Kbir belongs to the basin of the lower Lakkous (Figure 2), which is located at the limit of the meso-Rifan zone and constitutes the entirety of its eastern and northeastern edge. The structuring of the region is part of the Alpine tectonic evolution that marks the Rif range, the dominant Meso–Cenozoic and Mio–Plio–Quaternary lands record the different structures that mark the major Alpine phase: folds, thrust layers, overlaps, and fracturing [33,34]. In this area, a relatively calm structure is found, consisting of gray marls of the Upper Cretaceous (Senonian mainly), white marls and marl limestones from Eocene, and gray marls with sandstone banks of the Oligo–Miocene (sandstone “Larachian”). Shreds of “Numidian” sandstones associated with their clay base can be found locally.

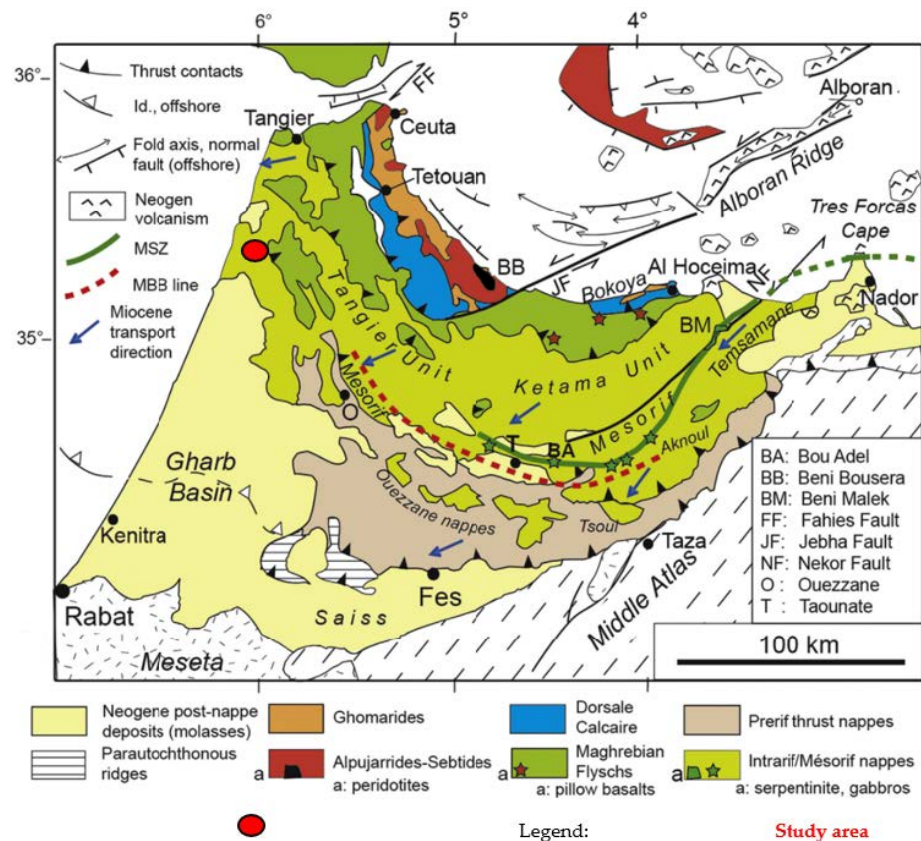


Figure 2. Simplified geological map of the Rif belt [35].

### 2.3. Rainfall Characteristics

The RR410 road is subject to several instabilities, particularly following the exceptional wetter period that Morocco experienced in winter 2008 and 2013 [36]. Due to the geographical proximity of the study area to the city of Larache, and especially the similarity of the rainfall patterns of the two areas, the data from the Larache weather station, regularly monitored, were used to understand the climatology of the study area. Figure 3 shows a graph of the monthly accumulation of precipitation calculated according to meteorological available readings from 1980 to 2009.

This figure shows that the wettest seasons are from October to April, where the number of days ranges from 5 to 12. This shows the important rainfall during autumn and winter in this region. The rainfall data used came from the analysis of the Larache station provided by the National Meteorological Services. The parameters provided below (Table 1) come from the statistical analysis of a sample of around thirty years (1980 to 2009).

Table 1. Maximum daily rainfall recorded in the station of Larache.

Precipitation Recurrence Interval	Maximum Daily Rainfall
5 years	71 mm
10 years	83 mm
20 years	95 mm
50 years	110 mm
100 years	121 mm

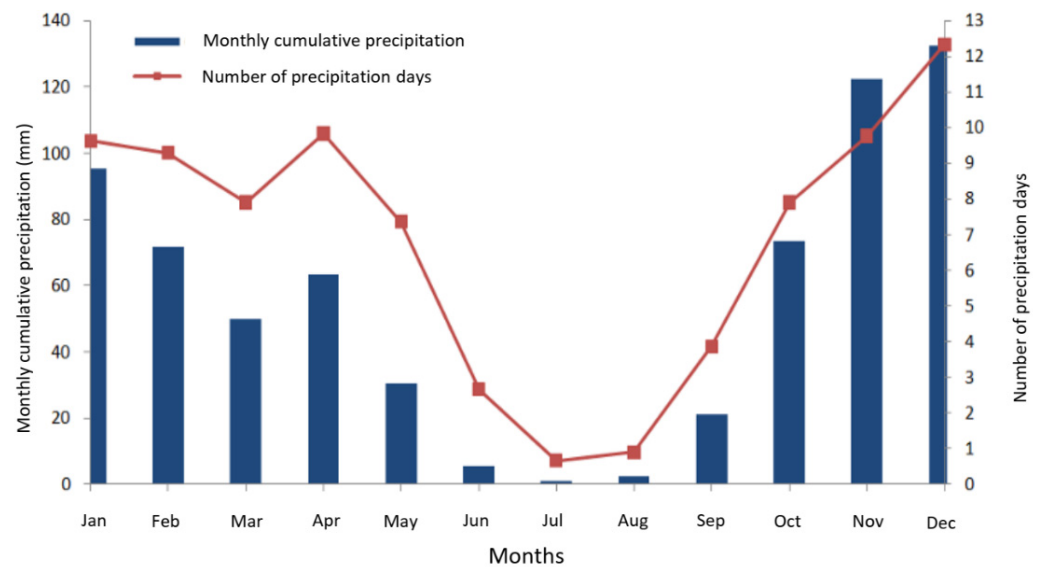


**Figure 3.** Monthly precipitation at Larache station (from 1980 to 2009).

#### 2.4. Hydrological Parameters

Field data were collected during field visits carried out in May 2014. They made it possible to observe the flow of water and the natural outlets. During these surveys, the pedology, land use, and slope of the watersheds near the road were identified to determine the share of infiltration and runoff.

The soils along the road are mainly clay–marly. These soils are very sensitive to erosion and often not very permeable, especially in the event of intense rainfall. The nature of the soil also conditions the plant cover. It is generally noted that the vegetation is mainly composed of grassy and forest surfaces. The watershed runoff coefficients are calculated as follows:

- The basin is broken down into subbasins with the same runoff capacity (same plant cover and same type of soil) for which the runoff coefficients are calculated.
- The surface runoff coefficients of these subbasins are weighted.

$$C_{eq} = \frac{\sum_i C_i x A_i}{\sum_i A_i} \quad (1)$$

where:

$C_{eq}$ : catchment runoff coefficient;

$A_i$ : surface of subbasin  $i$ ;

$C_i$ : Runoff coefficient of sub-watershed  $i$ .

The B.C.O.E.M. table provides the runoff coefficients according to the characteristics of the watersheds. The values of the coefficients are adapted to the reality on the ground and readjusted according to the morphology of the basins crossed and the size of the slopes intercepted. For the estimation of the project flows, and given that the totality of the identified watersheds are all smaller than 20 km<sup>2</sup>, the calculation of their peak flows is performed using the rational method [37–39] as follows:

$$Q_T = \frac{C_r x I_T x A}{3.6} \quad (2)$$

where:

$C_r$ : runoff coefficient;

$A$ : surface of the basin in km<sup>2</sup>;

$I_T$ : rain intensity in mm/h.

The intensity is calculated using the formula below:

$$I(T) = a(T) \times Tc^{-b(T)} \quad (3)$$

With:

$I$ : intensity in mm/h;

$a$  &  $b$ : Montana coefficients (Given in Table 2);

**Table 2.** Montana  $a$  and  $b$  parameters for a concentration time between 6 min and 730 min (Data taken from the meteorological data of Larache Station).

Return Period	Montana Coefficient $a$	Montana Coefficient $b$
2 years	4.688	0.662
5 years	6.586	0.674
10 years	7.878	0.680
20 years	9.130	0.685
50 years	10.760	0.690

$Tc$ : time of concentration.

For geographical and topographical reasons, rainfall data from the Larache station were applied to the project area.

In the Moroccan context, the usual choice of the return period in the hydraulic works of a road is 25 years. The Montana parameters of this return period, not appearing in the table above, have been interpolated from the available values. The time of concentration was estimated by averaging the Kirpich and VanTeChow formulas as follows:

Kirpich formula:

$$tc = 1/52 \times \left( \frac{L \times 1000}{\sqrt{P}} \right)^{0.77} \quad (4)$$

VanTeChow formula:

$$tc = 0.123 \times \left( \frac{L}{P^{0.5}} \right)^{0.64} \times 60 \quad (5)$$

With:

$Tc$ : time of concentration in minutes;

$L$ : length of the longest hydraulic path in km;

$P$ : slope in m/m.

### 3. Observed Disorders

#### 3.1. Kilometric Point 23

The road, as shown in Figure 4c,d, is located on a natural slope, which is relatively low (Around 15°).

A landslide occurred on the platform for about 140 linear meters (Figure 4a,b). This caused its departure downstream as well as its subsidence. On the upstream side (Figure 4c), several marked flows (leaving significant traces on the slope) were observed. These arrivals infiltrate through the voids created by the digging of the ground by runoff water and affect the platform, especially in the absence of drainage devices. The deposits of solid matter resulting from the gully of the ground are seated at the bottom of the drainage ditch. On the platform (Figure 4d), the observed subsidence reached a depth of 3 m. The repetitive collapses were at the origin of the cut of the circulation on several occasions. Previous interventions have consisted of regularly reloading the platform to maintain traffic.

### 3.2. Kilometric Point 48

The road, as shown in Figure 5c,d is in mixed profile. The section affected by the disorders totals a linear of approximately 300 m (Figure 5a,b).

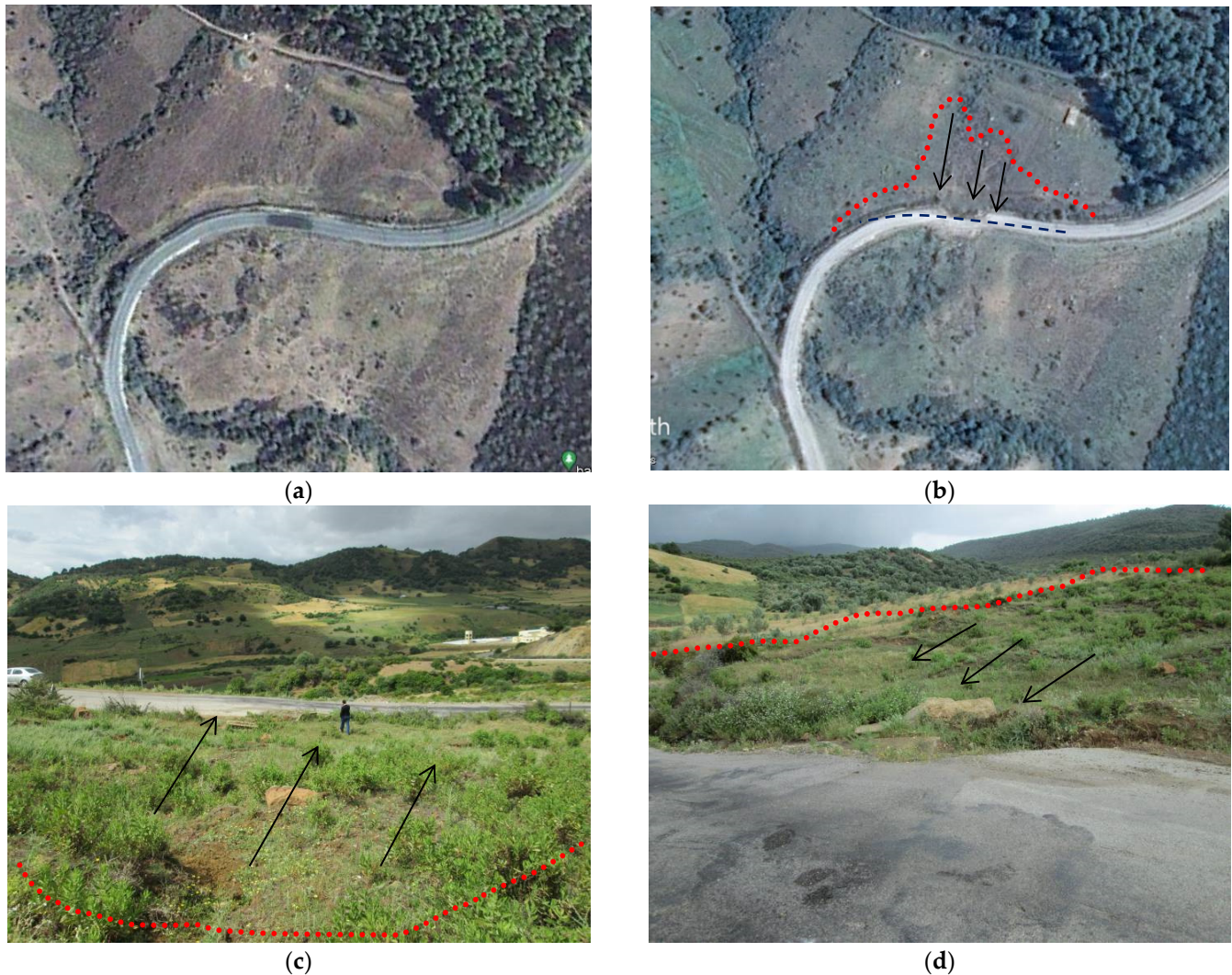
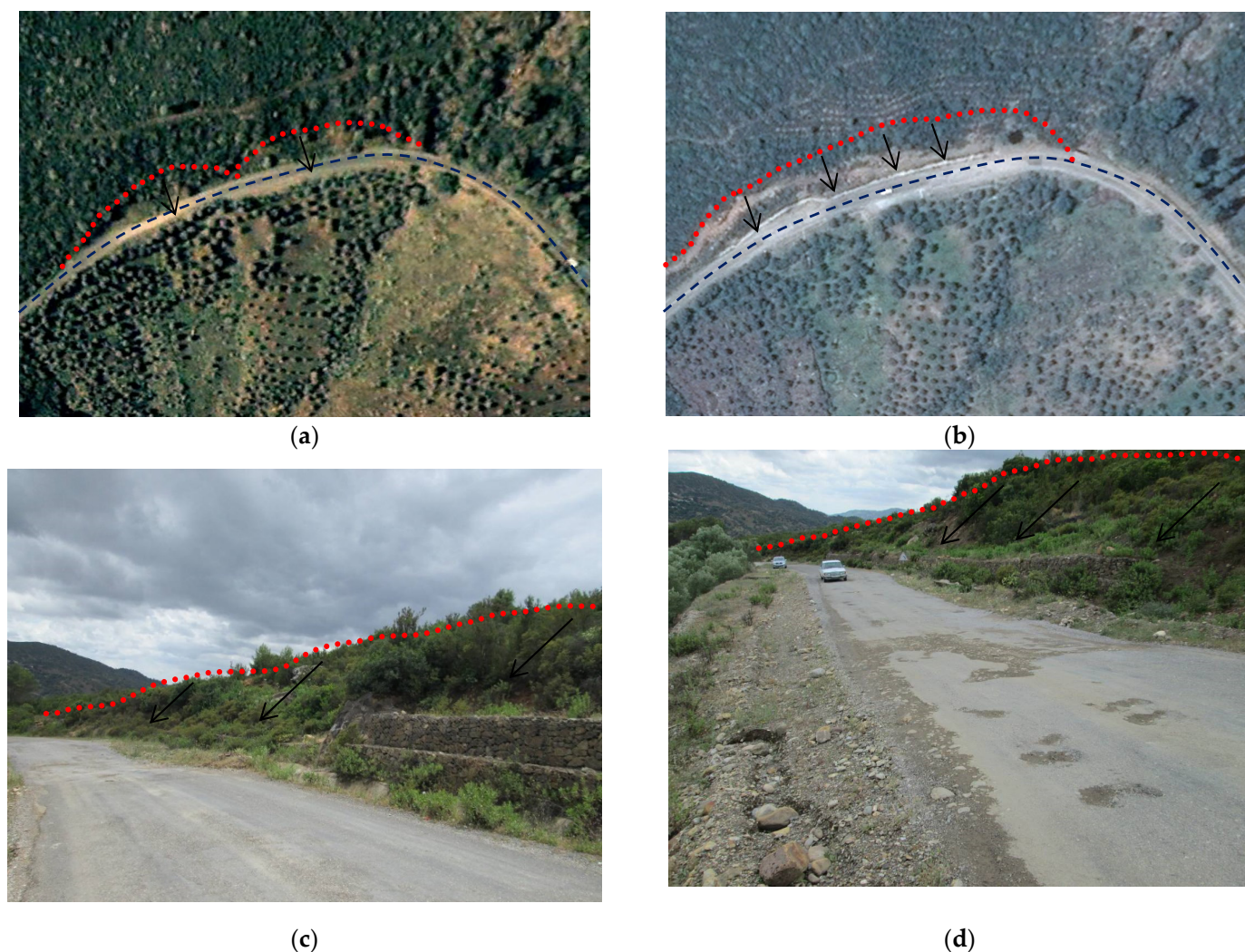


**Figure 4.** Illustration of the disorders observed at kilometric point 23: (a) Google Earth view of the road taken in October 2011; (b) Google Earth view of the departure of the platform taken in February 2014; (c) image taken from upstream (May 2014); (d) picture taken on the platform (May 2014).

At the excavated side (Figure 5c), setbacks associated with a fall of blocks and stones were visible. This was treated using a gabion wall, without any intervention on the slope. The bottom ditches are blocked by solid deposits from the gullies of the upstream slope. On the platform (Figure 5d), the observed subsidence reached a depth of 3 m. This corresponds to talweg zones, where the existing hydraulic structures (culvert type), were diagnosed as insufficient. Also, the two existing hydraulic structures are partly blocked by solid transport. In the absence of drainage, runoff water therefore infiltrates through the body of the road embankment and causes deterioration of the road. On the downstream side, a major crack affected the shoulder and caused the start of its departure. Part of the embankment was reinforced by a gabion wall, the other part by a masonry wall, which was broken in places by the force of the interstitial pressures. The repetitive collapses were at the origin of the cut of the circulation on several occasions.



Legend:

..... Landslide boundary    - - - Road axis    → Direction of ground movement

**Figure 5.** Illustration of the disorders observed at kilometric point 48: (a) Google Earth view of the disorder observed taken in January 2003; (b) Google Earth view of the departure of the platform taken in March 2014; (c) picture taken from upstream (May 2014); (d) picture taken on the platform (May 2014).

#### 4. General Methodology

The methodology followed, as shown in Figure 6, consisted of carrying out various tasks, according to thoughtful steps, to identify the problem and provide suitable solutions for the resolution of the disorders and the rehabilitation of the road. In order to optimize costs of repair work as much as possible, “earthmoving” type solutions are generally preferred. If these do not provide the desired stability, heavier solutions are then necessary. In addition, computer-aided drafting is of major importance because it makes it possible to rapidly project solutions and proceed with the necessary iterations to converge towards the final solution.

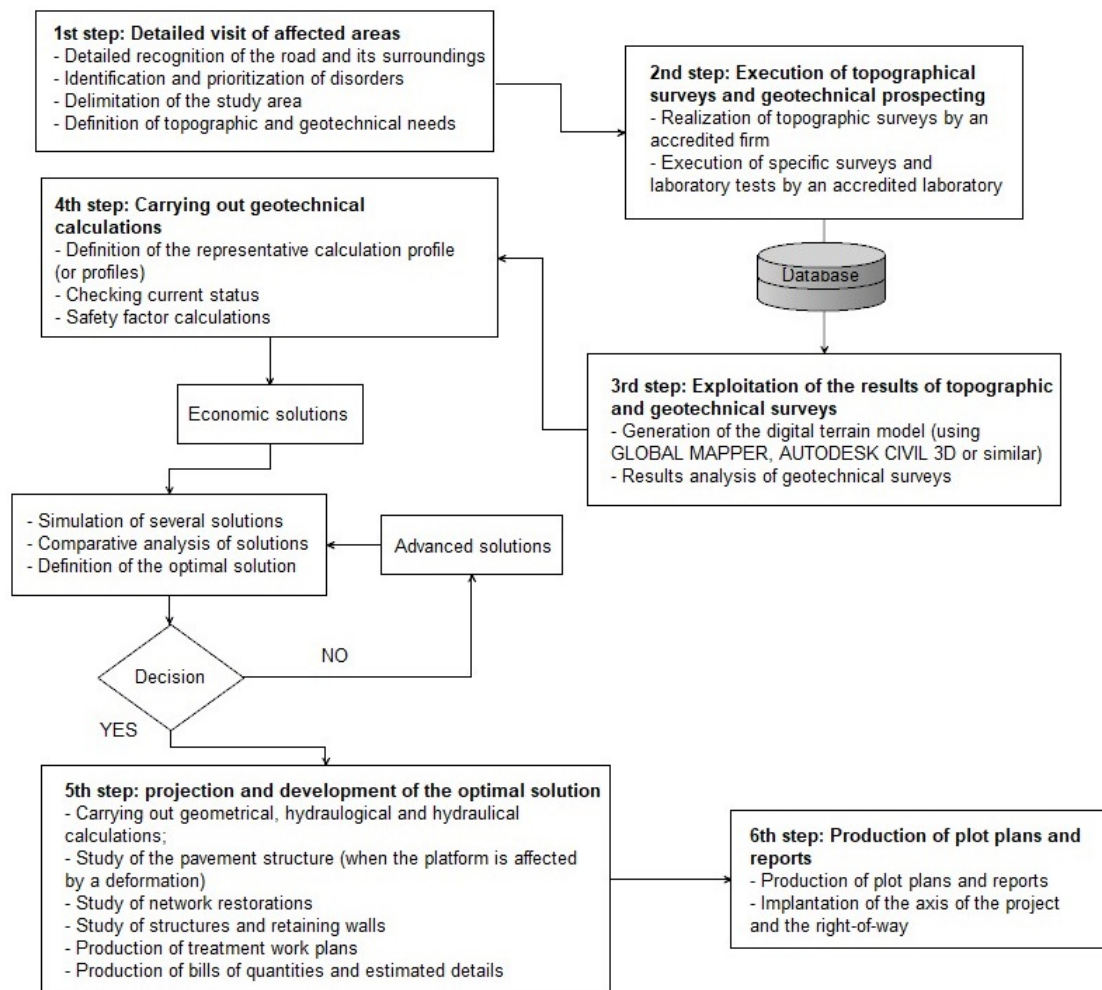


**Figure 6.** Flowchart of the detailed methodology followed to carry out this study.

## 5. Field Investigations

### 5.1. Topographic Works

Topographic studies were carried out by a topography engineering office. They were compiled using the requirements of the National Agency for Land Conservation, Cadaster, and Cartography and attached to the General Leveling of Morocco and the Lambert System. They consisted of the execution of various works as detailed below:

- Ground survey of the strip quoted at 1/1000: consisted of establishing a strip quoted at 1/1000 lifted on the ground, showing all the visible details in the defined strip (buildings, networks, roads, tracks, ridge lines, thalwegs, etc.);
- 1/500-rated plan: this task concerns hydraulic structures, crossroads, and restoration of various networks;
- Survey implementation: they were installed at X, Y, and Z coordinates, at the locations defined by the geotechnical program;
- Implementation and materialization of the project axis: this task is usually programmed at the end of the project and consists of the implementation and materialization of sustainable landmarks of the axis by the topographical team.

Topographic ground surveys were used to establish digital terrain models related to the two study areas (Figure 7).

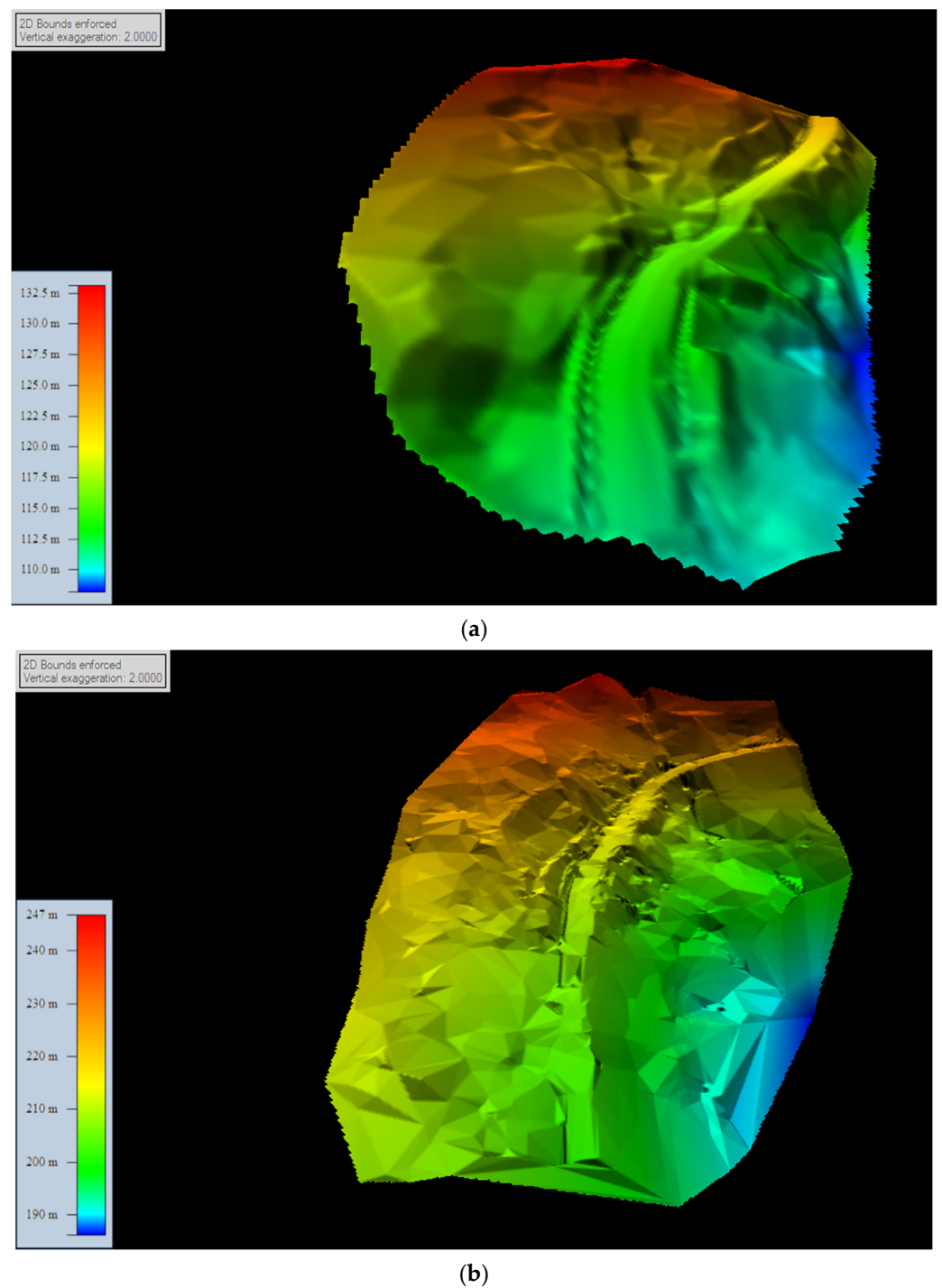
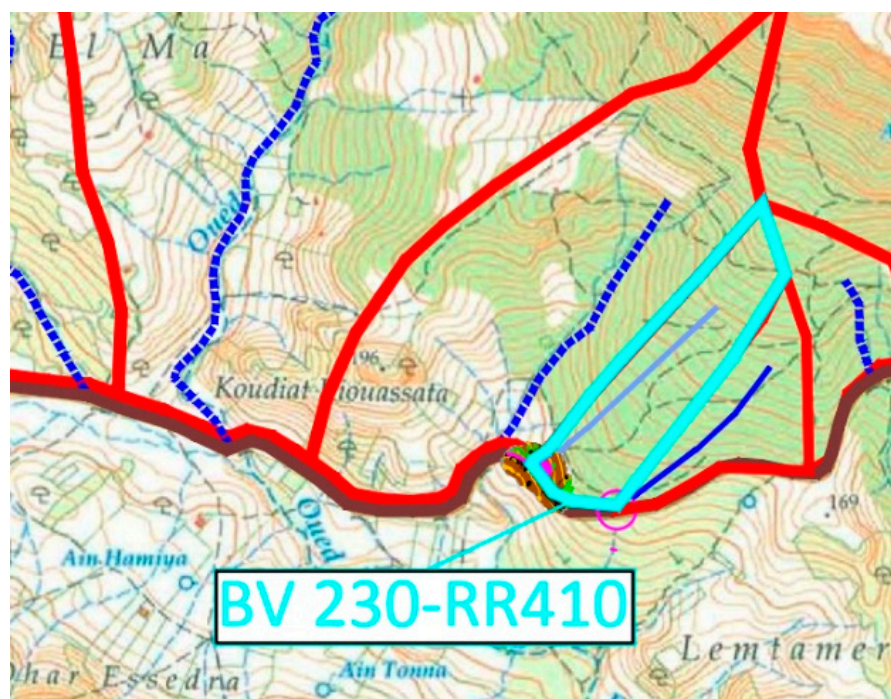


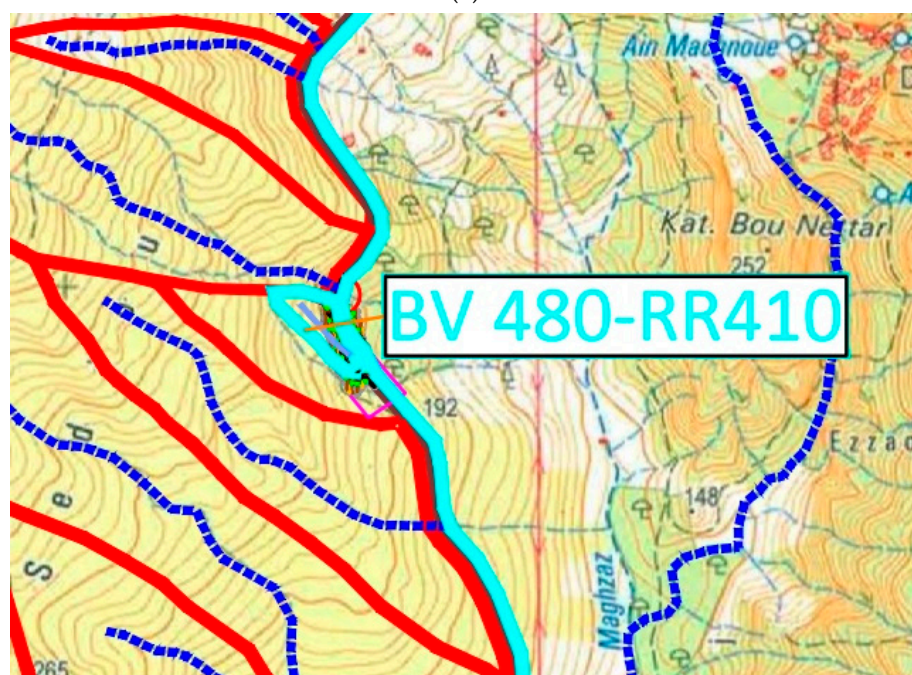
**Figure 7.** Digital terrain model of the two study areas, developed from topographic survey data: (a) kilometric point 23; (b) kilometric point 48.

### 5.2. Hydrological Investigations

Several runoff flows derived from exterior watersheds intercept the road. Based on the 1/50.000 topographic maps, the watersheds were delineated and the corresponding boundaries are shown in the Figure 8. These flows correspond to small and medium-sized watersheds (less than 10 km<sup>2</sup>). They are restored by hydraulic structures such as gutters or intercepted by ditches.



(a)



(b)

Legend:   
——— RR 410 road - - - - - Drain   
——— Watershed ——— Sub-watershed

**Figure 8.** Illustration of watershed delineation on a topographic map at a scale of 1/50,000: (a) kilometeric point 23; (b) kilometeric point 48.

Flow restoration is generally not completely transparent. The low impact on flows becomes significant when a rare and violent meteorological event occurs.

The hydraulic damage observed on the embankments (cut or fill) of the road sections inspected can be essentially summed up as follows:

- Clogging of lateral water structures;
- Inadequate hydraulic openings for OH and grooves;
- Low flow velocity (too low gradient) leads to lack of self-cleaning of drains and promotes solids buildup;
- Inadequate capture of crest outflow;
- The embankment body is inadequately drained.

In addition, the slopes are subject to climatic aggressions (rain, wind) that can lead—in the absence of sufficient vegetation cover to stabilize soils and depending on the overall context (nature of the soil, geometry of the slope, intensity and frequency of precipitation)—to a gradual departure of soil particles (gullying), then to its erosion. These phenomena gradually lead to the obstruction of the gutters and ditches located below, but also of the hydraulic crossing structures. When an extreme event occurs, or an event with a return period greater than that warranted by the initial design, the structure intended to restore the flow is no longer able to contain the entire park. The runoff water then overflows onto the road, infiltrates voids in the road embankment, or stagnates upstream of the hydraulic structure, leading to deterioration of the embankment, of the pavement, or even the hydraulic and concrete structures.

### 5.3. Geotechnical Investigations

At kilometric point 23 of the RR410 road, several investigations have been performed to examine the nature of the land in place. These consisted of the implementation of several surveys, as detailed below:

- On the upstream side: a 20 m cored survey, equipped with a piezometer;
- On the platform: a core sampling with measurement of the pressuremeter's characteristics [40];
- Downstream side: three (3) dynamic penetrometer tests [41].

The analysis of the borehole logs and the pressiometric characteristics measured onsite allows for distinguishing the following lithological sequence:

- From 0 to 7 m depth: a first layer essentially formed of gravelly silts, with limiting pressures ranging from 0.49 to 1.03 MPa and pressure moduli ranging from 0.95 to 3.64 MPa;
- From 7 to 17 m depth: the ground is constituted of sandy silts, having limit pressures varying from 1.4 to 1.36 MPa and pressiometric modules between 3.1 and 13.11 MPa.

These field surveys were also used to obtain some intact samples for laboratory tests. The summary of those different tests as well as the classification of the facies encountered are provided in Table 2.

At kilometric point 48 of the RR410 road, the in site geotechnical campaign consisted of the following surveys:

- On the cut side: a 20 m deep core sampling;
- On the platform: a core sampling with measurement of the pressuremeter's characteristics [41];
- Downstream side: three (3) dynamic penetrometer drillings [42], up to the refusal.

The analysis of the borehole logs and the pressiometric characteristics measured onsite allows for differentiation of the following formations:

- From 0 to 5 m depth: a first layer of gravelly silt with limiting pressures of 0.78 to 1.11 MPa and pressure moduli varying from 2.67 MPa to 6.38 MPa;
- From 5 to 14.5 m depth: a second layer of friable shale with limiting pressures varying from 1.53 to 3.43 and pressure moduli between 2.86 and 5.45 MPa.

In the same way, the summary of laboratory tests as well as the classification of the facies encountered are provided in Table 3.

**Table 3.** Geotechnical properties of facies found at the kilometric points 23 and 48.

Properties Value	Used Standard	Unit	Kilometric Point 23		Kilometric Point 48	
			Upper Layer	Bottom Layer	Upper Layer	Bottom Layer
Dmax	NF P 94-056 [43]	mm	63	25	63–80	40–63
Particle size analysis						
<80 $\mu\text{m}$	NF P 94-056 [43]	%	40.9–42.9	53.4–53.2	33.5–36.2	11–23.6
>2 mm		%	22.7–25.1	7–7.2	45.5–47.2	40–68
>50 mm		%	4.2–5.9	-	1.4–3.4	0–5.7
PI	NF P 94-051 [44]	%	10–12	17–18	20–22	11–25
Natural density ( $\gamma_h$ )	NF P 94-053 [45]	KN/m <sup>3</sup>	18.7	18.5	18.8–19	18.8–19.3
Shearing parameters						
Cohesion (c')	NF P 94-071 [46]	KPa	16–21	35–38	15–24	15–27
Friction angle ( $\phi'$ )		°	22–24	30–31	30–35	29–35
GMTR classification	Moroccan guide for road earthworks [40]		C1A1	A2	C1A2 /C1B6	B5 /C1B6

## 6. Slope Stability Analysis

### 6.1. General Calculation Assumptions

The safety factors used for stability calculations, based on conventional final weights, are  $FS > 1.5$  under static conditions and  $FS > 1$  under dynamic conditions. Additionally, a load of 10 KN/m<sup>2</sup> distributed over the road was considered. Furthermore, mainly in fine soils (marl, silt, etc.), it makes more sense to consider soil saturation rather than specific water levels.

Based on the regulatory seismic classification issued by the General Direction of Roads, the study area belongs to Zone M4. The assumed acceleration value for the long-term slope stability dynamic analysis is  $0.20 \times g$ . The retained calculation profile corresponds to the most unfavorable zone not only in terms of project height (embankment or cut), but also in terms of cover's thickness.

### 6.2. Initial Conditions

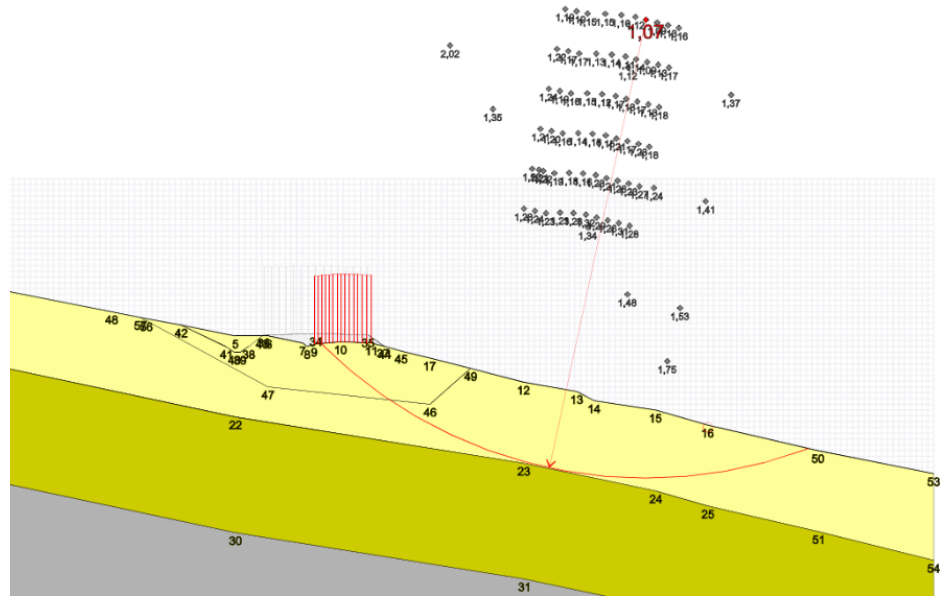
At the kilometric point 23 of the RR410 road, the use of mechanical parameters measured in the laboratory lead to acceptable slip safety coefficients ( $F > 1.5$ ). However, the road in this area experienced a major disorder with the departure of the platform. For this, the mechanical parameters of the subgrade were calibrated, using a back analysis, in order to have a safety coefficient close to or equal to 1 ( $F \approx 1$ ), i.e., at the stable equilibrium of the ground, as shown at the Figure 9a. The calibration of the model was judged as satisfying because it faithfully reproduced the current mode of rupture, i.e., a circular slide that has swept away the road.

The Table 4 summarizes geotechnical parameters resulting from this approach.

**Table 4.** Geotechnical parameters retained following the model calibration at kilometric points 23 and 48.

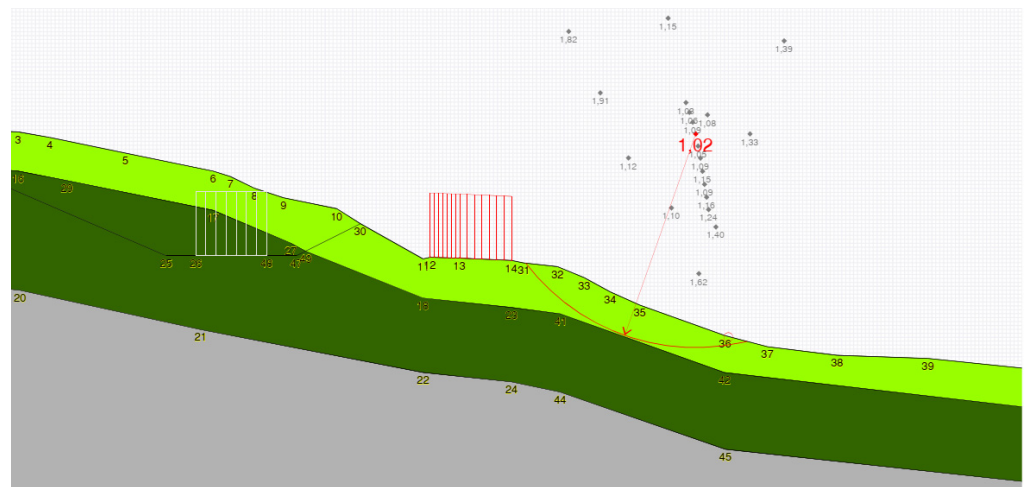
Location	Layers	Thickness (m)	Density (KN/m <sup>3</sup> )	Cohesion (KN/m <sup>2</sup> )	Friction Angle (°)
Kilometric point 23	Clay loam	7	18	10	15
	Sandy loam	10	18.7	18	22
	Substrate	Infinite	Infinite	Infinite	Infinite
Kilometric point 48	Gravelly loam	5	18	12	16
	Friable shale	9.5	18.4	16	20

**Fmin=1.07**



(a)

**Fmin=1.02**



(b)

**Figure 9.** Calibration of geotechnical parameters: (a) kilometric point 23; (b) kilometric point 48.

These parameters are indeed lower than those measured in the laboratory. This is probably due to the sample disturbance during sample recovery or during the setting for the shear tests. Also, the non-representativeness of the recovered samples could also be the origin of this problem. It should be noted that a 60% saturation was introduced in the first layer to consider the insufficiency of the existing hydraulic structure. In fact, the estimated capacity flow of the current hydraulic structure is  $0.7 \text{ m}^3/\text{s}$ , whereas the project flow for a return period of 25 years is equal to  $2.5 \text{ m}^3/\text{s}$ .

At kilometric point 48 of the RR410 road, the same problem was found. The mechanical parameters of the subgrade were also calibrated, using a back analysis, in order to have a safety coefficient close to or equal to 1 ( $F \approx 1$ ). Figure 9b shows the results of the initial state calibration. Those parameters, as shown in Table 4, are also lower than those measured in the laboratory. As explained above, this situation may be due to sample disturbance during sample recovery or during setting of the shear tests. In addition, the

non-representativeness of the recovered samples could also be at the origin of this problem. A 50% saturation was also introduced in the first layer to reflect the stagnation of water upstream of the platform, which infiltrates into the surface layers causing saturation of the latter. These are visible on the reinforcement wall located downstream of the road platform.

### 6.3. Result and Discussion

Once the initial situation was calibrated, the appropriate solutions for improving the stability of the road were simulated.

For kilometric point 23, the mode of damage caused involved the purging and replacement of the platform, as shown on Figure 10a,b, over the entire damaged area. The restoration of the original road geometry, involving the respect of the original red line, was necessary to rehabilitate in sustainable way the road.

To stabilize the road, calculations were used to determine several necessary actions, including reconstructing the platform to its initial geometry, selecting a 4.5 m thick embankment for the purge with a minimum friction angle of  $33^\circ$  and a density of  $20 \text{ KN/m}^3$  that is insensitive to water and has a very low percentage of fine particles. The purge and substitution inclination must be set according to the natural ground slope and oriented outside the degraded area. Additionally, a drainage trench and several drainage spurs spaced 10 m apart on the upstream side of the platform were constructed to collect infiltration water, and a draining base was installed for the platform to relieve interstitial pressures and drain possible water from the upstream side. The shoulders were concreted to limit water infiltration towards the embankment's body, and drainage outside the landslide area must be upgraded by increasing the opening of the existing upstream hydraulic structure. The actions considered essential are presented in a typical cross-section provided in Figure 10c. In addition, the excavation scheduled under the platform required the detour of traffic during the works. Since the geometry of the excavation determines the temporary deviation, a stability calculation was carried out. It shows a safety coefficient  $F = 1.2$  in the temporary phase, for a slope of the excavation equal to  $2H/1V$ , as shown in Figure 10d. With a view to limiting possible complications during the works, it was recommended to realize the excavation and replacement of the subgrade outside the rainy period.

At kilometric point 48, the optimal and sustainable solution that emerged from the analysis of the topographical, geometrical, and geotechnical constraints was to deviate the route, anchoring the platform in cuttings, under the same conditions of ground saturation. Circular slide stability calculations have shown that the road deviation is stable when the platform is anchored at 25 m from the current road axis. In fact, although the worst-case safety coefficient does not meet the stability requirements, the first slip circle that passes through the new platform has a safety coefficient of  $F_s > 1.5$  (Figure 11a,b). The old platform acts as a foot stop for the new one. A second stability calculation was also carried out to define the slope of the cuttings. The safety coefficient obtained is acceptable ( $F_s = 1.5$ ). The slope necessary for stability, as shown at Figure 11c,d, must be equal to  $2.5H/1V$ . Various measures were implemented to ensure stability and prevent landslides. These measures include realigning the road to anchor the new platform in the cuttings, constructing a three-bed gabion wall to act as a pebble trap and prevent erosion and falling debris, and implementing measures to collect and drain runoff and infiltration. These included concreting the shoulders, channeling pavement flow with beads, and installing water chutes, drainage trenches on the upstream side, and draining spurs spaced at 10 m intervals to collect infiltration water. Additionally, the hydraulic structure at the beginning of the rectification project was replaced with a new one capable of recovering runoff water, water collected by the draining spurs, and water from the drainage trench. These provisions aimed to enhance stability, promote proper drainage, and prevent future landslides as summarized in Figure 11e.

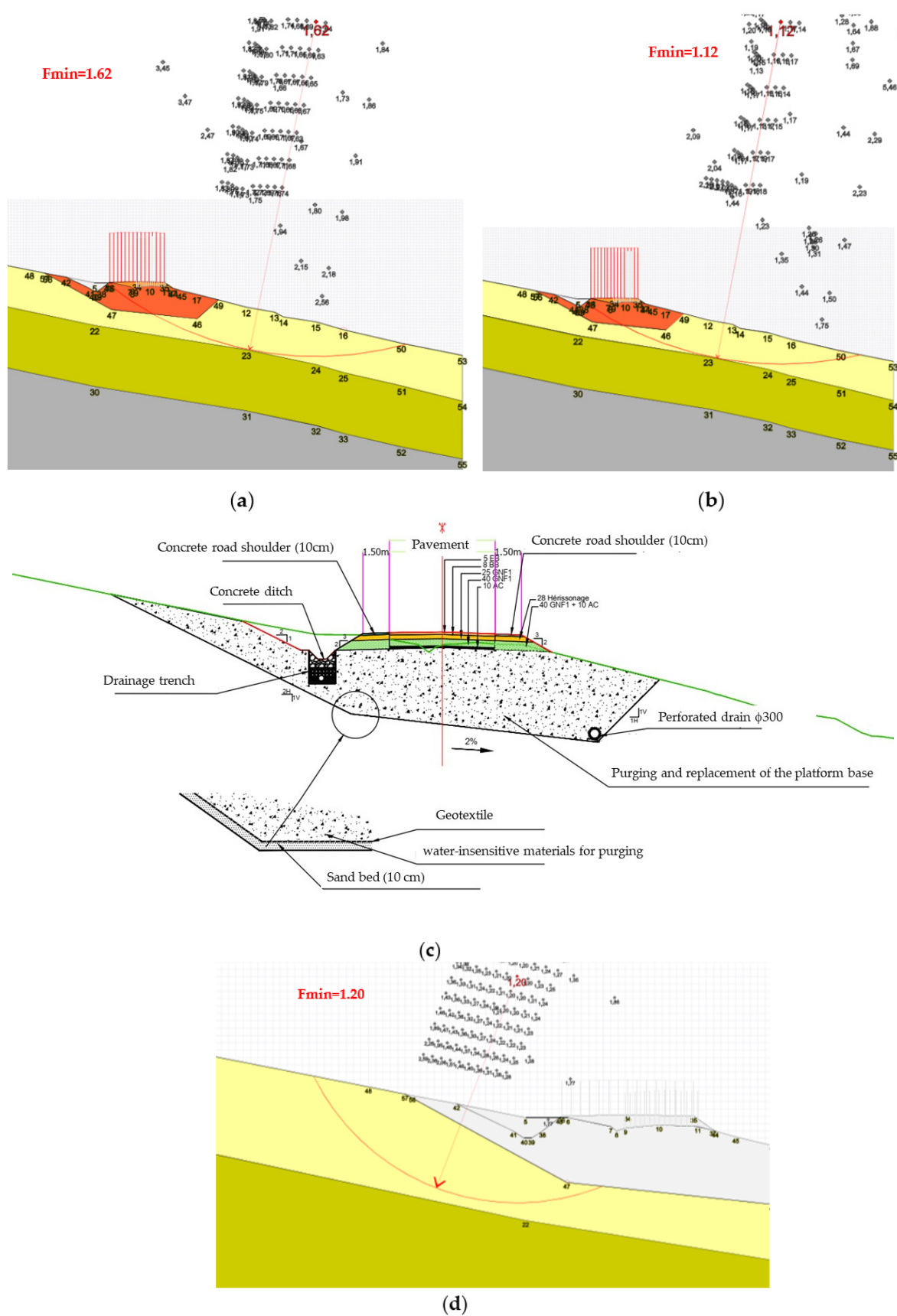


**Figure 10.** Results of the stability simulation at kilometeric point 23: (a) static condition; (b) dynamic condition; (c) typical cross-section of the adopted solution; (d) simulation of the temporary excavation stability.

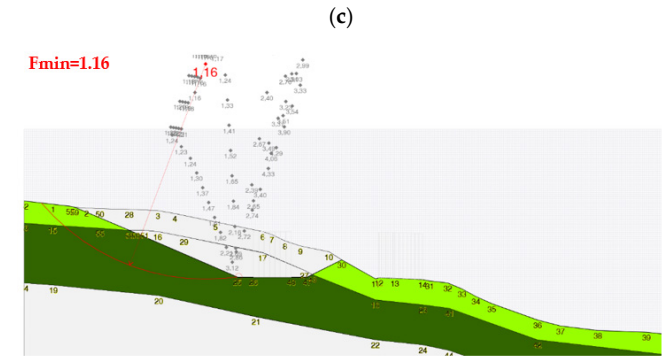
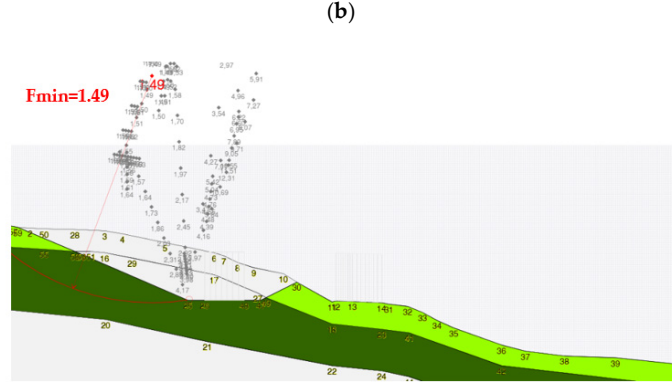
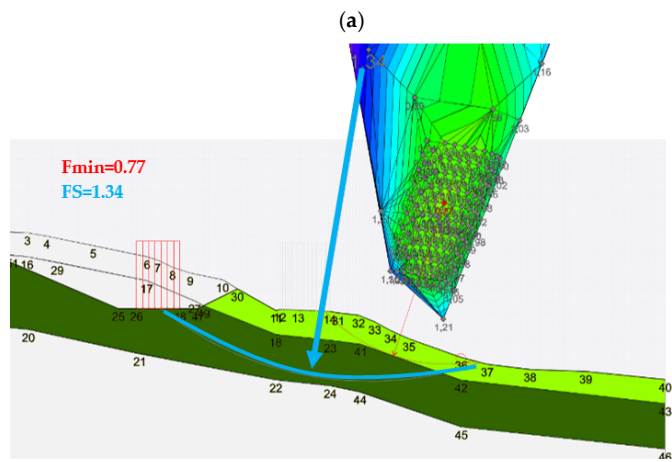
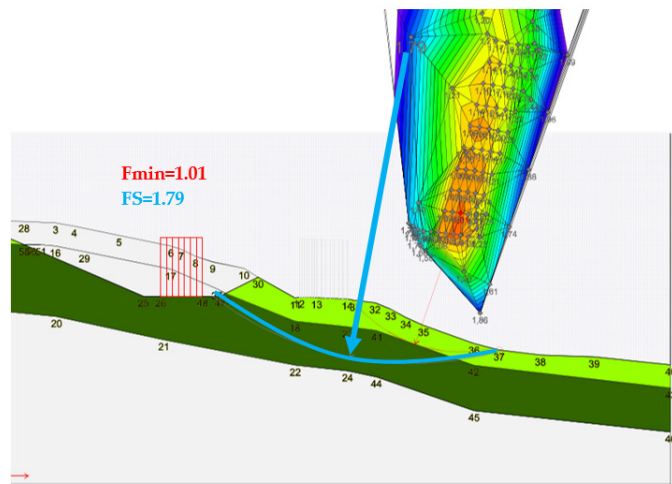
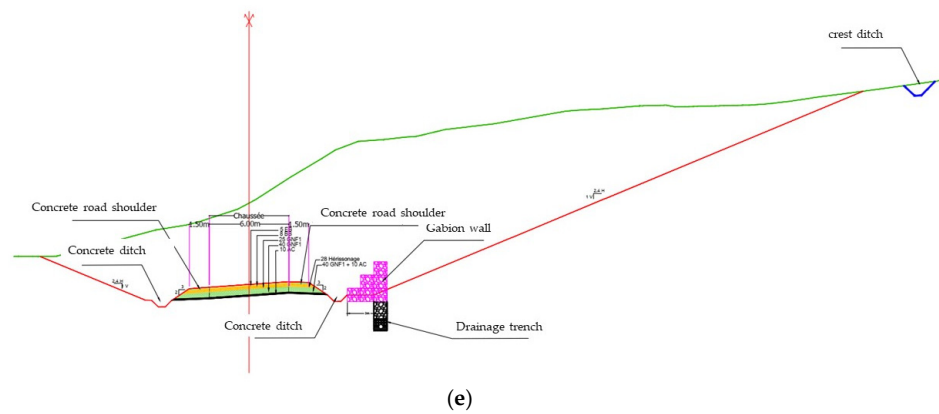


Figure 11. Cont.



**Figure 11.** Results of the stability simulation at kilometric point 48: (a) static condition; (b) dynamic condition; (c) static condition of the excavated side; (d) dynamic condition of the excavated side; (e) typical cross-section of the adopted solution.

### 7. Execution of Works and Status after Completion

For carrying out the works, a local company was hired, for several reasons. Firstly, local companies have a better understanding of the local environment, including ground and climate conditions, which enables them to handle any challenges that may arise during the work process. Secondly, local companies are often cost-effective as they do not have to incur additional costs associated with traveling to the final location. This can result in more competitive rates for their services. Moreover, communication with a local company can be more direct and efficient since they are located nearby. This can help to ensure that the work is carried out as per requirements, and any issues can be addressed promptly. Finally, by hiring a local company, supporting the local economy and helping to create jobs for the local community can be insured. This can have a positive impact on the local community and can be an essential aspect of corporate social responsibility.

If the road has not experienced any problems since the completion works in 2018 (Figure 12a–d), this is hard evidence that the mitigation measures were effective.

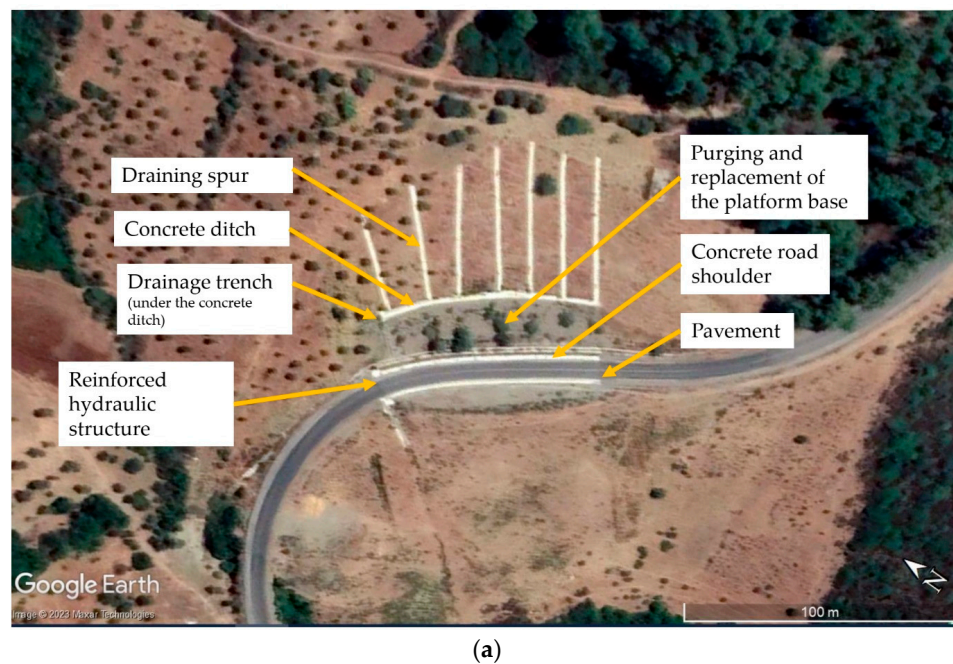
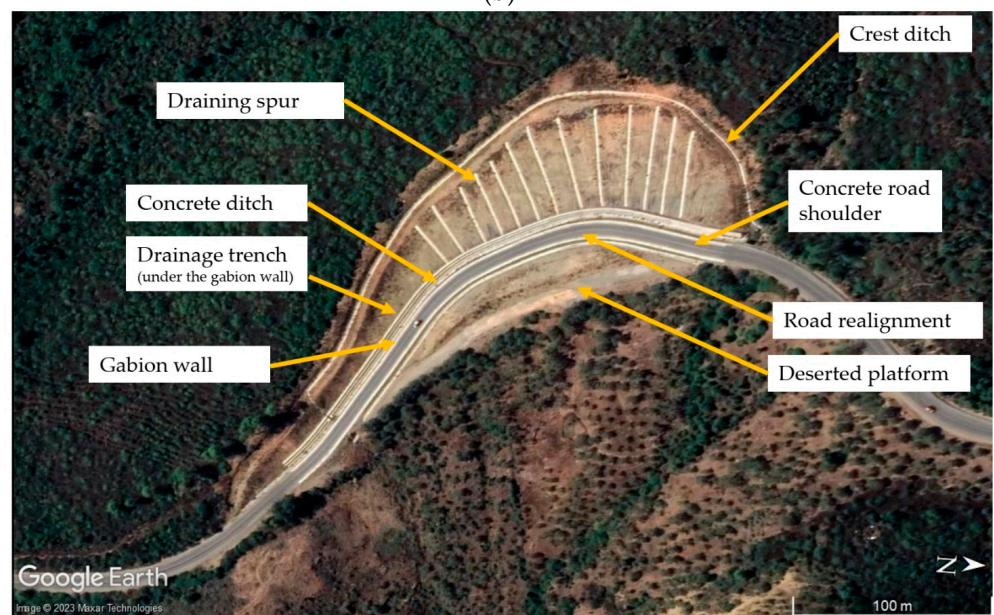


**Figure 12.** Cont.



(b)



(c)



(d)

**Figure 12.** Situation after completion of works: (a) Google Earth view of the kilometric point 23, taken in July 2022; (b) picture of kilometric point 23 taken in January 2022; (c) Google Earth view of the kilometric point 48, taken in January 2022; (d) picture of kilometric point 48, taken in January 2022.

## 8. Conclusions

This work aimed to share the Moroccan experience in dealing with landslides, a common occurrence in a structurally complex area. The key objective was to highlight the importance of understanding the failure mechanism and choosing the appropriate processing methods. Geological, geotechnical, and hydraulic specialists play a vital role in these studies, from developing an initial state to calibrating input data for simulations, ending with the definition of the constructive provisions.

This manuscript emphasizes the need for critical analysis of field data and test results, as even accredited laboratory tests may fail to reflect reality due to sample reworking during preparation or testing. In summary, this work focuses on the significance of a multidisciplinary approach and strict quality control measures in landslide studies.

Finally, earthwork solutions can be a more cost-effective, flexible, environmentally friendly, and durable option compared to reinforced concrete solutions for the treatment of landslides. They are more readily available and easier to transport and install, adaptable to the specific needs of a mountainous site, have lower environmental impact, and can be just as durable as reinforced concrete solutions. In summary, they are sustainable, easy-to-implement solutions that create local jobs.

**Author Contributions:** Conceptualization, O.I.; methodology, O.I.; software, O.I. and M.A.; validation, M.A.; formal analysis, O.I.; investigation, O.I.; resources, O.I. and M.A.; data curation, O.I.; writing—original draft preparation, O.I.; writing—review and editing, O.I., M.A., M.B. and M.Q.; visualization, O.I.; supervision, M.A. and M.Q.; project administration, M.A. and M.Q.; funding acquisition, M.A. All authors have read and agreed to the published version of the manuscript.

**Funding:** This work received no external funding.

**Data Availability Statement:** Data available upon request from the authors.

**Acknowledgments:** The authors express their gratitude to the reviewers for their valuable feedback, which led to significant improvements in the manuscript. Special thanks go to Y. Benyahya, A. El Krimi Idrissi, and W. Haddoun for their support in this work.

**Conflicts of Interest:** The authors declare no conflict of interest.

## References

1. Hungr, O.; Leroueil, S.; Picarelli, L. The Varnes Classification of Landslide Types, an Update. *Landslides* **2014**, *11*, 167–194. [[CrossRef](#)]
2. Guo, Z.; Chen, L.; Yin, K.; Shrestha, D.P.; Zhang, L. Quantitative Risk Assessment of Slow-Moving Landslides from the Viewpoint of Decision-Making: A Case Study of the Three Gorges Reservoir in China. *Eng. Geol.* **2020**, *273*, 105667. [[CrossRef](#)]
3. Petrucci, O. Landslide Fatality Occurrence: A Systematic Review of Research Published between January 2010 and March 2022. *Sustainability* **2022**, *14*, 9346. [[CrossRef](#)]
4. Haque, U.; da Silva, P.F.; Devoli, G.; Pilz, J.; Zhao, B.; Khaloua, A.; Wilopo, W.; Andersen, P.; Lu, P.; Lee, J.; et al. The Human Cost of Global Warming: Deadly Landslides and Their Triggers (1995–2014). *Sci. Total Environ.* **2019**, *682*, 673–684. [[CrossRef](#)]
5. Yazidi, M.; Benziane, F.; Yazidi, A.; Nabih, K.; Eloutassi, N. Gestion des instabilités de terrain au Maroc (cartographie et sécurité) [Management of landslide risks in Morocco (cartography and security)]. *Int. J. Innov. Appl. Stud.* **2017**, *21*, 25–36.
6. Mohamed, Y.; Noureddine, E.; Khadija, N.; Hadi, H.A.; Abdelaziz, Y.; Fouad, B. Gestion Des Risques Majeurs Au Maroc: Les Instabilités De Terrain. *Eur. Sci. J. ESJ* **2017**, *13*, 46–59. [[CrossRef](#)]
7. Chuaiwate, P.; Jaritngam, S.; Panedpojaman, P.; Konkong, N. Probabilistic Analysis of Slope against Uncertain Soil Parameters. *Sustainability* **2022**, *14*, 14530. [[CrossRef](#)]
8. Bishop, A.W. The Use of the Slip Circle in the Stability Analysis of Slopes. *Géotechnique* **1955**, *5*, 7–17. [[CrossRef](#)]
9. Wubalem, A. Comparison of General Limit Equilibrium Methods for Slope Stability Analysis. *Ethiop. J. Nat. Comput. Sci.* **2022**, *2*, 271–290. [[CrossRef](#)]
10. Cai, F.; Ugai, K. Discussion: Slope Stability Analysis by Finite Elements. *Géotechnique* **2001**, *51*, 653–654. [[CrossRef](#)]
11. Rotaru, A.; Bejan, F.; Almohamad, D. Sustainable Slope Stability Analysis: A Critical Study on Methods. *Sustainability* **2022**, *14*, 8847. [[CrossRef](#)]
12. Keskin, M.S.; Kezer, S. Stability of MSW Landfill Slopes Reinforced with Geogrids. *Appl. Sci.* **2022**, *12*, 11866. [[CrossRef](#)]
13. Baba, K.; Bahi, L.; Ouadif, L.; Akhssas, A. Slope Stability Evaluations by Limit Equilibrium and Finite Element Methods Applied to a Railway in the Moroccan Rif. *Open J. Civ. Eng.* **2012**, *2*, 27–32. [[CrossRef](#)]

14. Göktepe, F.; Keskin, I. A Comparison Study between Traditional and Finite Element Methods for Slope Stability Evaluations. *J. Geol. Soc. India* **2018**, *91*, 373–379. [[CrossRef](#)]
15. Memon, M.Y. *A Comparison between Limit Equilibrium and Finite Element Methods for Slope Stability Analysis*; Missouri University of Science and Technology: Rolla, MI, USA, 2018. [[CrossRef](#)]
16. Khabbaz, H.; Fatahi, B.; Nucifora, C. Finite Element Methods against Limit Equilibrium Approaches for Slope Stability Analysis. In *Australia New Zealand Conference on Geomechanics*; Geomechanical Society and New Zealand Geotechnical Society: Wellington, New Zealand, 2012.
17. Nagy-Göde, F.; Török, Á.; Horváth-Kálmán, E. The Stability Analysis of a Steep Slope at a Lake; Hungary. In Proceedings of the 6th International Conference on Geotechnical and Geophysical Site Characterization (ISC2020), Online, 26–29 September 2021; Available online: <https://doi.org/10.53243/ISC2020-531> (accessed on 26 June 2023).
18. Rabie, M. Comparison Study between Traditional and Finite Element Methods for Slopes under Heavy Rainfall. *HBRC J.* **2014**, *10*, 160–168. [[CrossRef](#)]
19. Mansour, Z.S.; Kalantari, B. Traditional Methods vs. Finite Difference Method for Computing Safety Factors of Slope Stability. *Electron. J. Geotech. Eng.* **2011**, *16*, 1119–1130.
20. Igwe, O.; Fukuoka, H. The Effect of Water-Saturation on the Stability of Problematic Slopes at the Iva Valley Area, Southeast Nigeria. *Arab. J. Geosci.* **2015**, *8*, 3223–3233. [[CrossRef](#)]
21. Li, Y. A Review of Shear and Tensile Strengths of the Malan Loess in China. *Eng. Geol.* **2018**, *236*, 4–10. [[CrossRef](#)]
22. Zhang, S.; Xu, Q.; Hu, Z. Effects of Rainwater Softening on Red Mudstone of Deep-Seated Landslide, Southwest China. *Eng. Geol.* **2016**, *204*, 1–13. [[CrossRef](#)]
23. Ahmed, M.F.; Khan, M.S.; Raza, M.A.; Saqib, S.; Saadat, H. Slope failure analysis of havelian landslide, abbotabad pakistan. *Pak. J. Sci.* **2016**, *68*, 462–469.
24. Roccati, A.; Paliaga, G.; Luino, F.; Faccini, F.; Turconi, L. Rainfall Threshold for Shallow Landslides Initiation and Analysis of Long-Term Rainfall Trends in a Mediterranean Area. *Atmosphere* **2020**, *11*, 1367. [[CrossRef](#)]
25. Cevasco, A. Individuazione delle soglie pluviometriche di innesco di frane superficiali sul territorio comunale di genova: Il caso della val bisagno/evaluation of rainfall thresholds for triggering shallow landslides on the genoa municipality area (Italy): The case study of the bisagno valley. *Ital. J. Eng. Geol. Environ.* **2010**, *1*, 35–50. [[CrossRef](#)]
26. Aleotti, P. A Warning System for Rainfall-Induced Shallow Failures. *Eng. Geol.* **2004**, *73*, 247–265. [[CrossRef](#)]
27. Cannon, S.H.; Gartner, J.E.; Wilson, R.C.; Bowers, J.C.; Laber, J.L. Storm Rainfall Conditions for Floods and Debris Flows from Recently Burned Areas in Southwestern Colorado and Southern California. *Geomorphology* **2008**, *96*, 250–269. [[CrossRef](#)]
28. Sengani, F.; Mulenga, F. Influence of Rainfall Intensity on the Stability of Unsaturated Soil Slope: Case Study of R523 Road in Thulamela Municipality, Limpopo Province, South Africa. *Appl. Sci.* **2020**, *10*, 8824. [[CrossRef](#)]
29. Ait Lemkadem, A.; Michelot, J.-L.; Benkaddour, A.; Hanich, L.; Heddoun, O. Origin of Groundwater Salinity in the Draa Sfar Polymetallic Mine Area Using Conservative Elements (Morocco). *Water* **2022**, *15*, 82. [[CrossRef](#)]
30. Adiguna, G.A.; Wijaya, M.; Rahardjo, P.P.; Sugianto, A.; Satyanaga, A.; Hamdany, A.H. Practical Approach for Assessing Wetting-Induced Slope Failure. *Appl. Sci.* **2023**, *13*, 1811. [[CrossRef](#)]
31. Islam, M.A.; Islam, M.S.; Jeet, A.A. A Geotechnical Investigation of 2017 Chattogram Landslides. *Geosciences* **2021**, *11*, 337. [[CrossRef](#)]
32. Lazzari, M.; Gioia, D.; Anzidei, B. Landslide Inventory of the Basilicata Region (Southern Italy). *J. Maps* **2018**, *14*, 348–356. [[CrossRef](#)]
33. Martín-Martín, M.; Guerrero, F.; Hlila, R.; Maaté, A.; Maaté, S.; Tramontana, M.; Serrano, F.; Cañaveras, J.C.; Alcalá, F.J.; Paton, D. Tectono-Sedimentary Cenozoic Evolution of the El Habt and Ouezzane Tectonic Units (External Rif, Morocco). *Geosciences* **2020**, *10*, 487. [[CrossRef](#)]
34. El Hamdouni, I.; Ait Brahim, L.; El Mahsani, A.; Abdelouafi, A. The Prevention of Landslides Using the Analytic Hierarchy Process (AHP) in a Geographic Information System (GIS) Environment in the Province of Larache, Morocco. *Geomat. Environ. Eng.* **2022**, *16*, 77–93. [[CrossRef](#)]
35. Michard, A.; Mokhtari, A.; Lach, P.; Rossi, P.; Chalouan, A.; Saddiqi, O.; Rjimati, E.-C. Liassic Age of an Oceanic Gabbro of the External Rif (Morocco): Implications for the Jurassic Continent–Ocean Boundary of Northwest Africa. *Comptes Rendus Geosci.* **2018**, *350*, 299–309. [[CrossRef](#)]
36. Khaddor, I.; Achab, M.; Soumali, M.R.; Alaoui, A.H. Rainfall-Runoff Calibration for Semi-Arid Ungauged Basins Based on the Cumulative Observed Hyetograph and SCS Storm Model: Application to the Boukhalef Watershed (Tangier, North Western Morocco). *J. Mater. Environ. Sci.* **2017**, *8*, 3795–3808.
37. Hosseiny, H.; Crimmins, M.; Smith, V.B.; Kremer, P. A Generalized Automated Framework for Urban Runoff Modeling and Its Application at a Citywide Landscape. *Water* **2020**, *12*, 357. [[CrossRef](#)]
38. Şen, Z. Hydrological Methodology Evolution for Runoff Estimations at Ungauged Sites. *Water* **2023**, *15*, 702. [[CrossRef](#)]
39. Granata, F.; Gargano, R.; de Marinis, G. Support Vector Regression for Rainfall-Runoff Modeling in Urban Drainage: A Comparison with the EPA's Storm Water Management Model. *Water* **2016**, *8*, 69. [[CrossRef](#)]
40. GMTR. *Direction des Routes et de la Circulation Routière*. 2002. *Guide Marocain pour les Terrassements Routier. Fascicule 1*; Royaume du Maroc; Ministère de l'Équipement: Rabat, Morocco, 2002; 106p.

41. *NF P94-110*; Soil: Investigation and Testing. Recognition and Tests—Menard Pressuremeter Test. French Standards Association: Paris, France, 1991.
42. *NF P94-114*; Soil: Investigation and Testing. Recognition and Tests—Dynamic Penetration Test Type A. French Standards Association: Paris, France, 1990.
43. *NF-P94-056*; Soil: Investigation and Testing. Granulometric Analysis. Dry Sieving Method after Washing. French Standards Association: Paris, France, 1996.
44. *NF-P94-052-1*; Soil: Investigation and Testing. Atterberg Limit Determination. Part 1: Liquid Limit. Cone Penetrometer Method. AFNOR Editions: La Plaine Saint-Denis, France, 1995.
45. *NF-P94-053*; Soil: Determination of the Density of Fine Soils in the Laboratory—Cutting Kit. Mould and Water Immersion Methods. AFNOR Editions: La Plaine Saint-Denis, France, 1991.
46. *NF-P94-071-1*; Soil Investigation and Testing. Direct Shear Test with Shearbox Apparatus. Part 1: Direct Shear. French Standards Association: Paris, France, 1994.

**Disclaimer/Publisher's Note:** The statements, opinions and data contained in all publications are solely those of the individual author(s) and contributor(s) and not of MDPI and/or the editor(s). MDPI and/or the editor(s) disclaim responsibility for any injury to people or property resulting from any ideas, methods, instructions or products referred to in the content.